

Article

## Integrated Portable Polymerase Chain Reaction-Capillary Electrophoresis Microsystem for Rapid Forensic Short Tandem Repeat Typing

Peng Liu, Tae Seok Seo, Nathaniel Beyor, Kyoung-Jin Shin, James R. Scherer, and Richard A. Mathies

*Anal. Chem.*, **2007**, 79 (5), 1881-1889 • DOI: 10.1021/ac061961k • Publication Date (Web): 02 February 2007

Downloaded from <http://pubs.acs.org> on February 27, 2009

### More About This Article

Additional resources and features associated with this article are available within the HTML version:

- Supporting Information
- Links to the 18 articles that cite this article, as of the time of this article download
- Access to high resolution figures
- Links to articles and content related to this article
- Copyright permission to reproduce figures and/or text from this article

[View the Full Text HTML](#)



**ACS Publications**  
High quality. High impact.

# Integrated Portable Polymerase Chain Reaction-Capillary Electrophoresis Microsystem for Rapid Forensic Short Tandem Repeat Typing

Peng Liu,<sup>†</sup> Tae Seok Seo,<sup>‡</sup> Nathaniel Beyor,<sup>†</sup> Kyoung-Jin Shin,<sup>§</sup> James R. Scherer,<sup>‡</sup> and Richard A. Mathies<sup>\*,†,‡</sup>

UCSF/UC Berkeley Joint Graduate Group in Bioengineering, and Department of Chemistry, University of California, Berkeley, California 94720

A portable forensic genetic analysis system consisting of a microfluidic device for amplification and separation of short tandem repeat (STR) fragments as well as an instrument for chip operation and four-color fluorescence detection has been developed. The microdevice performs polymerase chain reaction (PCR) in a 160-nL chamber and capillary electrophoresis (CE) in a 7-cm-long separation channel. The instrumental design integrates PCR thermal cycling, electrophoretic separation, pneumatic valve fluidic control, and four-color laser excited fluorescence detection. A quadruplex Y-chromosome STR typing system consisting of amelogenin and three Y STR loci (DYS390, DYS393, DYS439) was developed and used for validation studies. The multiplex amplification of these 4 loci with 35 PCR cycles followed by CE separation and 4-color fluorescence detection was completed in 1.5 h. All the amplicons can be detected with a limit of detection of 20 copies of male standard DNA in the reactor. Real-world forensic analyses of oral swab and human bone extracts from case evidence were also successfully performed. Mixture analysis demonstrated that a balanced profile can be obtained even at a male-to-female template ratio of 1:10. The successful development and operation of this portable PCR–CE system establishes the feasibility of rapid point-of-analysis DNA typing of forensic casework, of mass disaster samples or of individuals at a security checkpoint.

Short tandem repeat (STR) assays have become an indispensable and routine technique in modern forensic casework since their first application in 1991.<sup>1</sup> Polymerase chain reaction (PCR)-based amplification of multiple STR loci followed by capillary

electrophoretic (CE) separation provides STR assays with high sensitivity and high discrimination power.<sup>2–4</sup> In addition to forensic identification, STR assays have found application in paternity testing, missing person investigations, human identification in mass disasters, evolution, and clinical diagnosis.<sup>5,6</sup> However, the limited capabilities of current genotyping technologies, which are time-consuming, labor-intensive, and expensive, have resulted in backlogs in forensic laboratories around the world. To address these issues, high-throughput and integrated instruments are needed to improve the data productivity. In addition, rapid and portable DNA typing devices that can provide on-site forensic analysis could be valuable in crime scene investigation and for law enforcement and security applications.

In the quest to produce portable, real-time analytical devices as well as high-throughput analyzers, microfabricated microfluidic analysis systems, so-called micro total analysis systems ( $\mu$ TAS), have attracted increasing attention due to their ability to integrate multiple molecular biology processes at the microliter to nanoliter scale in a single device. Since the inception of  $\mu$ TAS in 1990,<sup>7</sup> much progress has been made to miniaturize and integrate DNA analysis steps into a microchip format,<sup>8,9</sup> including DNA extraction,<sup>10–12</sup> PCR amplification,<sup>13,14</sup> and CE separation.<sup>15–17</sup> These technologies are now beginning to be translated to forensic applications.

\* Corresponding author. Phone: (510) 642-4192. Fax: (510) 642-3599. E-mail: rich@zinc.cchem.berkeley.edu.

<sup>†</sup> UCSF/UC Berkeley Joint Graduate Group in Bioengineering.

<sup>‡</sup> Department of Chemistry.

<sup>§</sup> On leave from: Department of Forensic Medicine, Yonsei University College of Medicine, Seoul 120-752, Korea.

- (1) Edwards, A.; Civitello, A.; Hammond, H. A.; Caskey, C. T. *Am. J. Hum. Genet.* **1991**, *49*, 746–756.
- (2) Gill, P.; Whitaker, J.; Flaxman, C.; Brown, N.; Buckleton, J. *Forensic Sci. Int.* **2000**, *112*, 17–40.
- (3) Chakraborty, R.; Stivers, D. N.; Su, B.; Zhong, Y.; Budowle, B. *Electrophoresis* **1999**, *20*, 1682–1696.

- (4) Butler, J. M. *J. Forensic Sci.* **2006**, *51*, 253–265.
- (5) Jobling, M. A.; Gill, P. *Nat. Rev. Genet.* **2004**, *5*, 739–751.
- (6) Butler, J. M. *Forensic STR Typing: Biology, Technology and Genetics of STR Markers*. 2nd ed.; Elsevier: New York, 2005.
- (7) Manz, A.; Graber, N.; Widmer, H. M. *Sens. Actuators B* **1990**, *1*, 244–248.
- (8) deMello, A. J. *Nature* **2006**, *442*, 394–402.
- (9) Dittich, P. S.; Tachikawa, K.; Manz, A. *Anal. Chem.* **2006**, *78*, 3887–3907.
- (10) Tian, H.; Huhmer, A. F.; Landers, J. P. *Anal. Biochem.* **2000**, *283*, 175–191.
- (11) Breadmore, M. C.; Wolfe, K. A.; Arcibal, I. G.; Leung, W. K.; Dickson, D.; Giordano, B. C.; Power, M. E.; Ferrance, J. P.; Feldman, S. H.; Norris, P. M.; Landers, J. P. *Anal. Chem.* **2003**, *75*, 1880–1886.
- (12) Bienvenue, J. M.; Duncalf, N.; Marchiarullo, D.; Ferrance, J. P.; Landers, J. P. *J. Forensic Sci.* **2006**, *51*, 266–273.
- (13) Wilding, P.; Shoffner, M. A.; Kricka, L. J. *Clin. Chem.* **1994**, *40*, 1815–1818.
- (14) Kopp, M. U.; de Mello, A. J.; Manz, A. *Science* **1998**, *280*, 1046–1048.
- (15) Paegel, B. M.; Emrich, C. A.; Wedemayer, G. J.; Scherer, J. R.; Mathies, R. A. *Proc. Natl. Acad. Sci. U.S.A.* **2002**, *99*, 574–579.
- (16) Emrich, C. A.; Tian, H.; Medintz, I. L.; Mathies, R. A. *Anal. Chem.* **2002**, *74*, 5076–5083.
- (17) Medintz, I.; Wong, W. W.; Berti, L.; Shio, L.; Tom, J.; Scherer, J.; Sensabaugh, G.; Mathies, R. A. *Genome Res.* **2001**, *11*, 413–421.

In 1997, Ehrlich's group demonstrated that a quadruplex STR system (*CSF1PO*, *TPOX*, *THO1*, *vWA*) could be separated with high accuracy in less than 2 min by microchip capillary electrophoresis.<sup>18</sup> More recent work in our group demonstrated the use of a 96-channel microfabricated capillary array electrophoresis device coupled to a four-color confocal fluorescence scanner for high-performance STR typing using both the PowerPlex 16 and AmpF/STR Profiler Plus multiplex PCR systems.<sup>19</sup> The separations were completed in less than 30 min with single-base resolution on 96 CE channels simultaneously. Although these systems heavily rely upon conventional off-chip sample preparation, they do indicate that chip-based CE technology is poised for application in forensic laboratories.

The on-chip integration of DNA sample amplification by PCR has also been demonstrated. An integrated PCR–CE microdevice consisting of a silicon reaction chamber attached to a glass CE analysis chip was developed in our laboratory in 1996 to amplify and analyze PCR products, providing rapid reaction times, low sample consumption, and potential on-chip integration with other analytical techniques.<sup>20</sup> Since then, great progress has been made in the development of PCR microdevices, including alternative chip formats (flow-through and stationary chamber), substrate materials (silicon, glass, and polymer), and heating methods (contact and noncontact heating).<sup>21,22</sup> However, most of these systems either require a high starting template concentration or are not suitable for integration with CE separation.

Based on the development of integrated PCR–CE microdevices by Lagally et al.,<sup>23–25</sup> a fully integrated portable PCR–CE microsystem was recently demonstrated for pathogen detection applications. The limit of detection for this system was 2–3 *Escherichia coli* cells, and the amplifications required only 20 min.<sup>26</sup> More recently, a nanoliter-scale microdevice was developed, that integrates the three Sanger sequencing steps: thermal cycling, sample purification, and capillary electrophoresis.<sup>27</sup> Building on this work, a four-lane integrated PCR–CE array microdevice was also demonstrated to amplify femtogram amounts of DNA followed by electrophoretic separation in less than 30 min.<sup>28</sup> These advances raise the possibility that these technologies can also be used for forensics whose stringent requirements include high efficiency and balanced amplification of multiple STR loci, reproducible electrophoretic separation under denaturing conditions, and high-sensitivity, four-color fluorescence detection.

Here we present the design and operation of a new PCR–CE microdevice for forensic STR analysis, as well as a new portable analysis instrument, which contains all the electronics and optics for temperature control, microfluidic manipulation, CE separation, and four-color fluorescence detection. To explore the utility of this system for forensic DNA typing, a quadruplex STR system was developed with amelogenin, a sex-typing marker, and three Y chromosome STR loci. As over 89% of violent offenses are committed by men,<sup>29</sup> Y-STR assays have a unique value in forensic DNA typing, particularly in sexual assault cases.<sup>6,30,31</sup> Due to the lack of recombination, Y-STR assays have also become a popular tool for paternity testing, evolutionary studies, and historical and genealogical research.<sup>6</sup> With this quadruplex Y-STR system, we evaluated the limit of detection of the portable PCR–CE microsystem as well as its ability to analyze forensic casework samples and to detect male DNA in a background of female DNA.

## EXPERIMENTAL SECTION

**Microdevice Design.** The microdevice contains two identical PCR–CE systems, symmetrically arranged on the 4-in. wafer (Figure 1A). The structure of each system is similar to the device developed in our group previously,<sup>26</sup> but the design has been adapted for the portable instrument. Each system consists of a 160-nL PCR chamber, an integrated heater, a four-point resistance temperature detector (RTD), two poly(dimethylsiloxane) (PDMS) microvalves, and a 7-cm-long CE separation channel. The PCR reactor region with the relative positions of the PCR chamber, heater, and RTD is shown in Figure 1B.

The microdevice is composed of a glass manifold, a PDMS membrane, a glass heater/channel wafer, and a glass RTD wafer (Figure 1C). The PCR chamber (bottom side of the heater/channel wafer) and the RTD (top side of the RTD wafer) are positioned next to each other after bonding. The microfabricated PCR heater is deposited on the top side of the heater/channel wafer and covers the PCR chamber and the RTD to facilitate thermal cycling under the control of the temperature feedback from the RTD. The PCR chamber contains three exits, two of which are connected to a loading reservoir and a vent reservoir, respectively, through microvalves for the sample loading. The last exit is coupled to a CE separation channel through a narrow injection channel. The glass manifold wafer actuates the PDMS microvalves for fluidic control.<sup>32</sup>

**PCR Heater Design.** The design of the microfabricated PCR heater is intended to create uniform heating over the entire PCR chamber and to facilitate fast thermal response times. In general, the edges of the heater show the most deviation from temperature set point due to the higher thermal dissipation. To adequately maintain the entire chamber volume at a single temperature and keep the thermal mass of the PCR system as low as possible, the thermal power at the extremities of the heater was increased to diminish the temperature deviation. The PCR heater was designed in an iterative process using computational simulation as a guide.

- (18) Schmalzing, D.; Koutny, L.; Adourian, A.; Belgrader, P.; Matsudaira, P.; Ehrlich, D. *Proc. Natl. Acad. Sci. U.S.A.* **1997**, *94*, 10273–10278.
- (19) Yeung, S. H. I.; Greenspoon, S. A.; McGuckian, A. B.; Crouse, C. A.; Emrich, C. A.; Ban, J.; Mathies, R. A. *J. Forensic Sci.* **2006**, *51*, 740–747.
- (20) Woolley, A. T.; Hadley, D.; Landre, P.; deMello, A. J.; Mathies, R. A.; Northrup, M. A. *Anal. Chem.* **1996**, *68*, 4081–4086.
- (21) Roper, M. G.; Easley, C. J.; Landers, J. P. *Anal. Chem.* **2005**, *77*, 3887–3894.
- (22) Zhang, C.; Xu, J.; Ma, W.; Zheng, W. *Biotech. Adv.* **2006**, *24*, 243–284.
- (23) Lagally, E. T.; Simpson, P. C.; Mathies, R. A. *Sens. Actuators B* **2000**, *63*, 138–146.
- (24) Lagally, E. T.; Medintz, I.; Mathies, R. A. *Anal. Chem.* **2001**, *73*, 565–570.
- (25) Lagally, E. T.; Emrich, C. A.; Mathies, R. A. *Lab. Chip* **2001**, *1*, 102–107.
- (26) Lagally, E. T.; Scherer, J. R.; Blazej, R. G.; Toriello, N. M.; Diep, B. A.; Ramchandani, M.; Sensabaugh, G. F.; Riley, L. W.; Mathies, R. A. *Anal. Chem.* **2004**, *76*, 3162–3170.
- (27) Blazej, R. G.; Kumaresan, P.; Mathies, R. A. *Proc. Natl. Acad. Sci. U.S.A.* **2006**, *103*, 7240–7245.
- (28) Liu, C. N.; Toriello, N. M.; Mathies, R. A. *Anal. Chem.* **2006**, *78*, 5474–5479.

- (29) U. S. Department of Justice, Federal Bureau of Investigation. *Crime in the United States*, 2005. <http://www.fbi.gov/ucr/05cius/index.html>.
- (30) Shewale, J. G.; Sikka, S. C.; Schneida, E.; Sinha, S. K. *J. Forensic Sci.* **2003**, *48*, 127–129.
- (31) Prinz, M.; Ishii, A.; Coleman, A.; Baum, H. J.; Shaler, R. C. *Forensic Sci. Int.* **2001**, *120*, 177–188.
- (32) Grover, W. H.; Skelley, A. M.; Liu, C. N.; Lagally, E. T.; Mathies, R. A. *Sens. Actuators B* **2003**, *89*, 315–323.

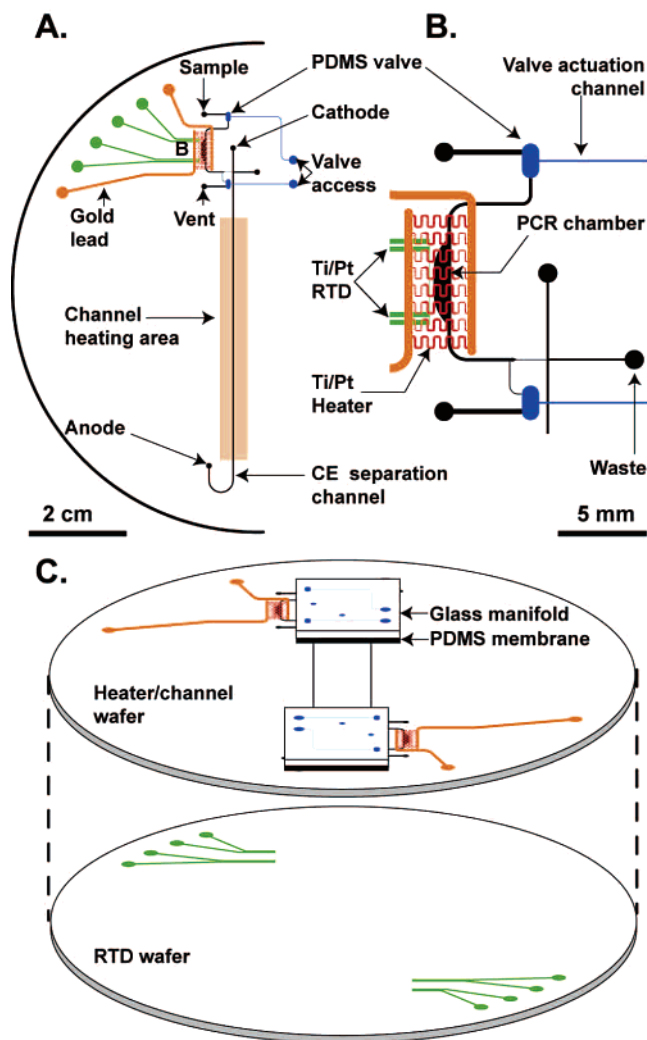


**Figure 1.** (A) Mask design for the PCR-CE microchip. The glass microchannels are indicated in black, the microfabricated RTD and electrodes are in green, the heater is shown in red, the gold leads of the heater are in gold, and the valves are drawn in blue. (B) Expanded view of the heater, RTD, PCR chamber, and CE injector. (C) Exploded view of the assembly of the PCR-CE microchip, showing the RTDs on the upper surface of the RTD wafer, as well as the glass microchannels etched in the lower surface and the heaters fabricated on the upper surface of the heater/channel wafer.

As shown in Figure 2, an optimized heater design contains eight serpentine heating elements connected to gold leads in parallel. The width of each heating element in the center region was set to  $140\ \mu\text{m}$ . Optimal heating distribution was achieved by narrowing the width to  $70\ \mu\text{m}$  on the ends of the central six heating elements, and to  $130\ \mu\text{m}$  on the outer two heating elements. Figure 2 (top) shows a color contour plot of the simulated temperature distribution of the PCR chamber at  $95\ ^\circ\text{C}$  using FEMLAB 2.3 (COMSOL, Inc., Burlington, MA). Using this design method, the temperature differences between the center and the edge of the PCR chamber were reduced to less than  $1\ ^\circ\text{C}$  in both the  $X$  and  $Y$  directions. Figure 2 (bottom) presents two typical PCR cycles. The temperature ramp rates can reach  $11.5\ ^\circ\text{C/s}$  for heating and  $4.7\ ^\circ\text{C/s}$  for cooling without any active cooling.

**Microfabrication.** The microfabrication process is similar to that described previously.<sup>25,26</sup> Briefly, to form the heater/channel

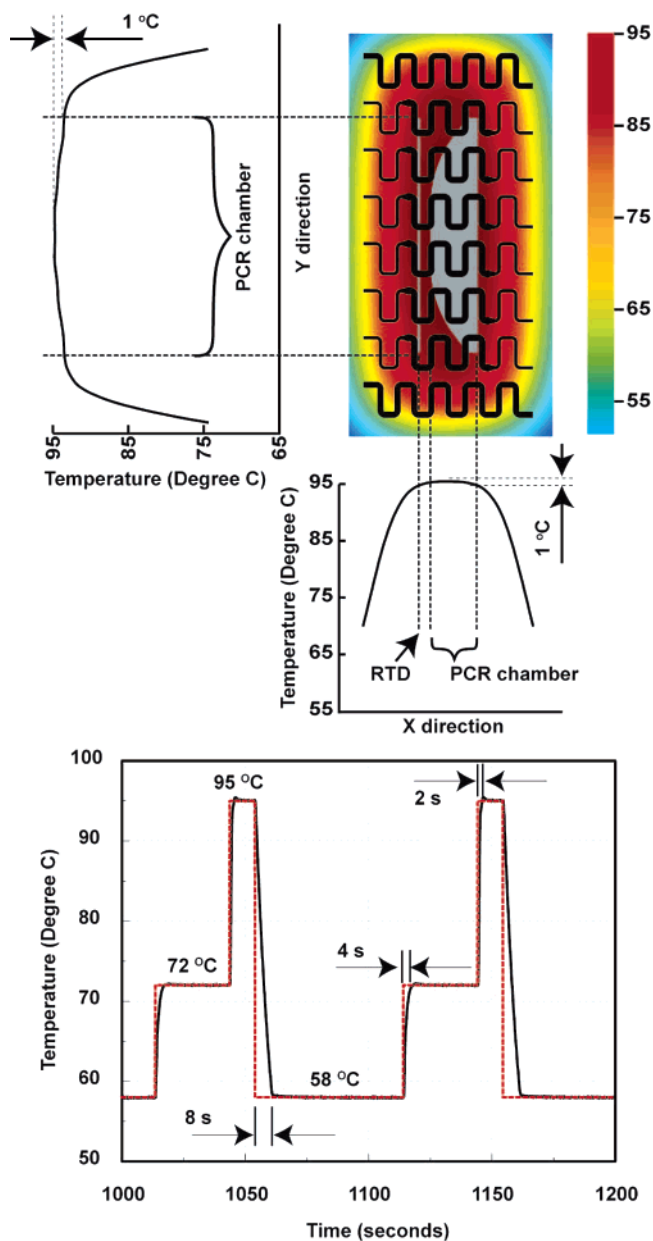


**Figure 2.** (Top) Color contour plot of the simulated temperature distribution of the PCR chamber layer at  $95\ ^\circ\text{C}$ . By varying the widths of the heating elements in the different regions of the heater, a uniform profile was achieved. The differences between the center and the edge of the heater are only  $1\ ^\circ\text{C}$ . (Bottom) Thermal cycling amplification profile. Black line shows the measured temperature from the RTD and red line is the set temperature. Temperature ramp rates were  $11.5\ ^\circ\text{C/s}$  for heating and  $4.7\ ^\circ\text{C/s}$  for cooling.

wafer, a  $550\text{-}\mu\text{m}$ -thick D263 glass wafer was coated with  $2000\text{-}\text{\AA}$  amorphous silicon on one side and  $200\text{-}\text{\AA}$  Ti and  $2000\text{-}\text{\AA}$  Pt on the other side. The channel pattern was photolithographically transferred to the amorphous silicon side, and then the sacrificial silicon was etched using  $\text{SF}_6$  in a parallel-plate reactive ion etching system creating a hard mask for subsequent glass etching. The exposed glass was etched to a depth of  $38\ \mu\text{m}$  in a 49% hydrofluoric acid bath. After etching, the photoresist and silicon were removed using acetone and  $\text{SF}_6$ , respectively. The integrated PCR heaters were fabricated on the Ti-Pt side of the same wafer. Using a backside contact aligner, a pattern defining the gold heater leads was photolithographically transferred to the surface. Gold was



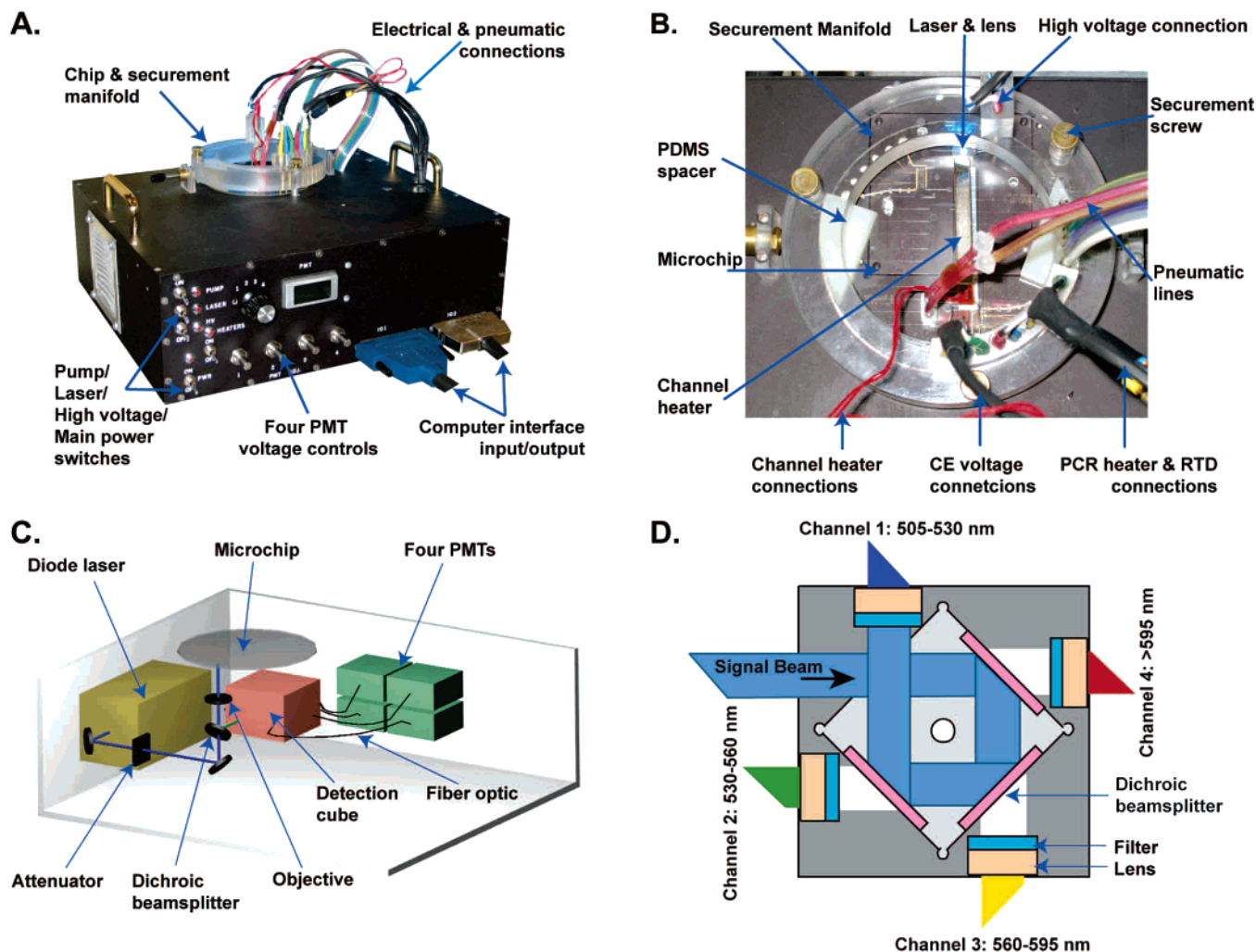


**Figure 3.** (A) Photograph of the portable PCR-CE system. The analysis system box has dimensions  $12 \times 10 \times 4$  in. (B) Closeup of the microchip and the manifold. A plexiglass manifold was used to fix the microchip in place and supply the electrical and pneumatic connections to the chip. (C) The schematic of confocal fluorescence detection system. (D) Expanded top view of the four-color detection cube.

electroplated onto the open Ti-Pt seed layer to a thickness of  $5 \mu\text{m}$  to form the heater leads. Photoresist was then removed, and the wafer was repatterned to define the heating elements. Using an ion beam etching system, the heating elements were etched into the Ti-Pt seed layer. Finally, holes were drilled using a CNC mill for via holes, fluidic reservoirs, and electrical and pneumatic access holes.

To form the RTD wafer, a  $700\text{-}\mu\text{m}$  D263 glass wafer coated with  $200\text{-}\text{\AA}$  Ti and  $2000\text{-}\text{\AA}$  Pt was patterned with photoresist and etched using hot aqua regia. To form the glass microchannels and PCR chambers, the RTD wafer and the heater/channel wafer were thermally bonded in a vacuum furnace at  $580^\circ\text{C}$  for 6 h. The glass manifold was fabricated from a  $700\text{-}\mu\text{m}$  D263 glass wafer using the same glass etching method described above and diced into  $23 \times 18$  mm pieces. The microvalves were assembled by cleaning the PDMS membrane in a UV-ozone cleaner for 1 min and then sandwiching the membrane between the bonded wafer stack and the glass manifold. This method results in a tight but reversible glass-PDMS bonding.

**Instrumentation.** The instrument used to perform analyses with the microdevice is shown in Figure 3A and B. The instrument contains a 488-nm, frequency-doubled diode laser, an optical

system for detecting four different fluorescence signals, pneumatics for the on-chip PDMS microvalves, electronics for PCR temperature control, and four high-voltage power supplies for CE. The weight of the instrument is 10 kg with a power consumption of 20 W, which can be supplied by a car battery. A LabVIEW graphical interface (National Instruments, Austin, TX) developed in-house was used to control the system through two DAQ boards (National Instruments).

The schematic of the detection system is shown in Figure 3C. The beam from the laser (Protera, Novalux Corp., Sunnyvale, CA) is reflected by a dichroic mirror (505DCXT, Chroma Technology Corp., Brattleboro, VT) into an attenuator that limits the power intensity of the laser beam to 4 mW (measured from the objective). Then, the attenuated beam is reflected by a second dichroic mirror (505DCXT), passes through a dichroic beam splitter (488DCSXPB, Chroma), and is focused into the channel in the microdevice with a custom-built objective (0.70-mm focal length in D263 glass, 0.88 NA). The returning fluorescent signal is collected by the objective and reflected into a four-color confocal detection cube by the dichroic beam splitter. As shown in Figure 2D, the detection cube separates fluorescent light into four distinct channels, blue (505–530 nm), green (530–560 nm), yellow (560–595 nm), and red

**Table 1. Locus Information, Dye Labeling, and Primer Sequences**

locus	repeat motif	dye label <sup>a</sup> and primer sequence (5' → 3')	9948 male standard DNA	
			repeat number	amplicon size (bp)
amelogenin		Fwd: [FAM-FAM]-CCCTGGGCTCTGTAAAGAA Rev: ATCAGAGCTTAAACTGGGAAGCTG	X, Y	106, 112
DYS390	[TCTG]- [TCTA] <sup>c</sup>	Fwd: [FAM-R6G]-CTGCATTTTGGTACCCCATATA Rev: GCAATGTGTATACTCAGAAACAAGG	24	171
DYS393	[AGAT]	Fwd: [FAM-TMR]-AACTCAAGTCCAAAAAATGAGG Rev: GTGGTCTTCTACTTGTGTCAATAC	13	123
DYS439	[GATA]	Fwd: [FAM-ROX]-ACATAGGTGGAGACAGATAGATGAT Rev: <u>GCCT</u> CAAGTGATCCACCCAAC <sup>b</sup>	12	191

<sup>a</sup> FAM, 5-carboxyfluorescein; R6G, rhodamine 6G; TMR, *N,N,N',N'*-tetramethyl-6-carboxyrhodamine; ROX, 6-carboxy-x-rhodamine. <sup>b</sup> The 5' G of the DYS439 reverse primer was added to promote adenylation. <sup>c</sup> Compound tetranucleotide repeat.

(>595 nm), by sequential reflection from a serial of dichroic beam splitters (595DCXR, 570DCXR, 537DCLP, Chroma). Fluorescent light is further filtered by a filter in each channel (Ch1, D520/26 m; Ch2, D550/20 m; Ch3, D580/26 m; Ch4, E600LP, Chroma). The filtered light is focused by an achromat lens (45208, Edmund Optics, Barrington, NJ) into an optical fiber (Newport Corp., Irvine, CA), the entry of which functions as a confocal pinhole and is provided with xyz adjustment, and then guided by an optical fiber to the desired PMT (H9306-03, Hamamatsu Corp., Bridgewater, NJ). The four signals are processed using an active 5-Hz, low-pass filter and collected at 10 Hz using the 16-bit DAQ board.

The microdevice is placed onto a recessed area on the top of the instrument and held in place with a plexiglass manifold. Two PDMS spacers are used to support the manifold and provide a soft contact to the microdevice. The manifold contains six spring-loaded pins pressed against the electrical pads on the device, providing the connections for sensing the RTD and powering the PCR heater. The manifold also contains Pt electrodes that are positioned within the reservoirs on the microchip for application of high voltages during CE. A thin-film heater, (9.2 Ω, Minco, Minneapolis, MN), sandwiched between the microchip and a magnet, is used to heat the CE separation channel. Flush contact between the magnetic heater and the chip is obtained by embedding a steel bar on the surface of the instrument.

The design of the electrical circuits for driving the RTD and heater is the same as presented earlier.<sup>26</sup> Briefly, a 4-mA current source powers the RTD through the outer set of leads, and the resulting voltage is sensed through the inner set. The signal is processed using an active low-pass filter at 5 Hz and then transferred to the DAQ board. Temperature control is accomplished through a proportion/integrator/differentiator module within the LabVIEW program, which outputs through the DAQ board to control the PCR heater power supply within the instrument.

The PDMS microvalves are controlled using vacuum or pressure supplied through pneumatic connections to the valve

access holes on the glass manifold. Eight pneumatic lines are available for fluidic control. Each line can be switched between vacuum (open valve) and pressure (closed valve) using a solenoid valve (H010E1, Humphrey, Kalamazoo, MI) controlled through the DAQ board. Pressure (4.5 psi) and vacuum (−8 psi) were separately supplied by two rotary pumps (G12/02−8-LC, Thomas, Sheboygan, WI) inside the instrument.

**Microdevice Preparation.** Before operation, the channels were first coated for 1 min with a dynamic coating diluted 1:1 with methanol (DEH-100, The Gel Co., San Francisco, CA) to minimize electroosmotic flow. The separation matrix, 5% (w/v) linear polyacrylamide with 6 M urea in 1× Tris TAPS EDTA (TTE) buffer, was loaded from anode reservoir with a syringe to fill the entire CE separation system. A prepared PCR mixture (10 μL) was pipetted into the sample reservoir. Vacuum applied at the vent reservoir moved the sample into the PCR chamber, and a gel–solution interface was formed at the end of the narrow injection channel. This interface functioned as a passive barrier to prevent the flow of reagents into the CE channels during thermal cycling. Using this method bubble-free loading of the PCR reactor was consistently achieved. After sample loading, the PDMS microvalves were closed by applying pressure to prevent hydrodynamic flow.

**PCR Amplification and Capillary Electrophoresis.** PCR amplifications were conducted from 9948 male and 9947A female genomic DNA (Promega commercial genomic DNA controls, Promega, Madison, WI), as well as two samples from forensic casework previously processed by the Palm Beach County Sheriff's Office. These casework samples were extracted from an oral swab and human bone, respectively, using the DNA IQ system (Promega), and then quantified using Quantiblot (Applied Biosystems, Foster City, CA) with Hitachi CCDBio (Hitachi, Alameda, CA) signal detection. All the DNA templates were also amplified in a traditional thermal cycler and analyzed in an ABI Prism 3100 genetic analyzer (Applied Biosystems) to obtain the

sizes of the allele fragments and validate corresponding on-chip results.

The quadruplex STR system included amelogenin and three Y-chromosome STR loci, DYS390, DYS393, and DYS439. Table 1 presents the PCR primers and associated dye labels, as well as the expected STR repeat numbers and amplicon lengths. The forward primers were labeled with energy-transfer dye cassettes developed in our group and described previously.<sup>33</sup> The 20- $\mu$ L PCR mixture prepared for each experiment was composed of gold STR buffer (50 mM KCl, 10 mM Tris-HCl (pH 8.3), 1.5 mM MgCl<sub>2</sub>, 0.1% Triton X-100, 160  $\mu$ g/mL BSA, 200  $\mu$ M each dNTP) (Promega), templates ranging from 0 to 50 copies in the 160-nL PCR chamber, primers, and FastStart Taq DNA polymerase (Roche Applied Science, Indianapolis, IN). The corresponding primer concentrations in the singleplex PCR amplifications were 150 nM for amelogenin, 80 nM for DYS390, 120 nM for DYS393, and 180 nM for DYS439, respectively. In the multiplex PCR reactions, the primer concentrations were adjusted to 150 nM for amelogenin, 150 nM for DYS390, 120 nM for DYS393, and 180 nM for DYS439. The final DNA polymerase concentration was 0.2 unit/ $\mu$ L in all experiments except for the analyses of male DNA in female DNA background, where the concentration was increased to 0.4 unit/ $\mu$ L. The thermal cycling protocol was composed of initial activation of the Taq polymerase at 95 °C for 4 min, followed by a PCR cycle of 95 °C for 10 s, 58 °C for 60 s, 72 °C for 30 s, and a final extension step for 2 min at 72 °C. For the singleplex reactions, 32 cycles were employed while 35 cycles were used for the multiplex.

Following microchip PCR amplification, the CE separation channel was heated to 70 °C using the channel heater. After the microvalve adjacent to the sample reservoir was opened, the amplified sample was electrophoretically injected into the CE system toward the waste by applying an electric field of  $\sim$ 100 V/cm while floating the anode and cathode. A separation field of 250 V/cm was then applied between the cathode and anode. In the first 5 s of the separation, a backbiasing field of 80 V/cm was applied at the sample and waste, which were floated for the remainder of the separation. Raw electropherograms were processed with BaseFinder 4.0. Processing procedures include baseline adjustment, cross-talk analysis, and convolution filtering. After each run, the glass manifold was removed, the PDMS membrane was replaced, and channels and chambers were cleaned using piranha (7:3 H<sub>2</sub>SO<sub>4</sub>/H<sub>2</sub>O<sub>2</sub>) to prevent run-to-run carryover contamination.

## RESULTS AND DISCUSSION

The quadruplex STR system for testing the portable four-color PCR-CE microsystem consists of the loci DYS390, DYS393, DYS439, and amelogenin. DYS390, DYS393, and DYS439 are members of the extended minimal haplotype loci, which play central roles in the current Y-STR DNA typing.<sup>34</sup> The haplotype diversity of these three loci is 0.9473 in the U.S. population. In addition to these three Y-STR loci, amelogenin, which codes for a protein found in tooth enamel, was employed. PCR amplification

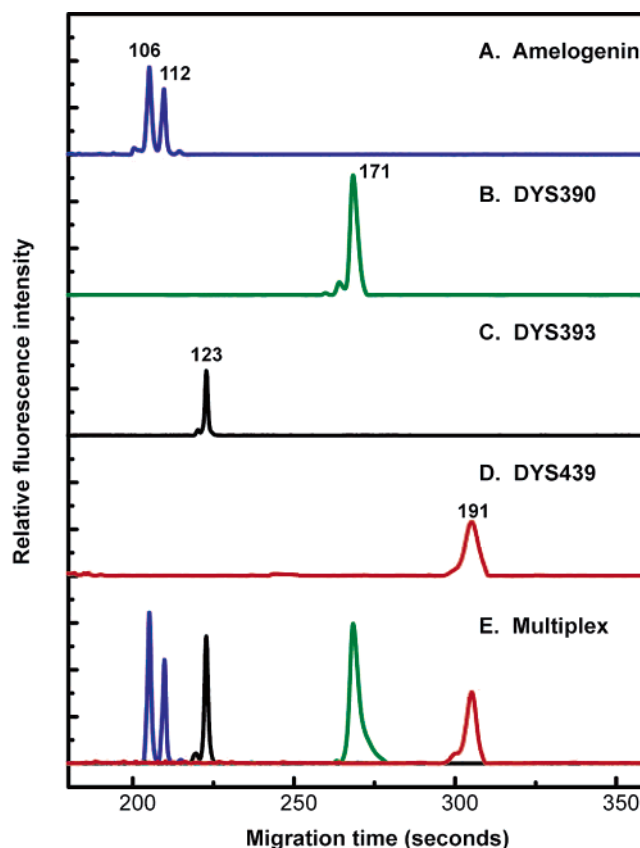


**Figure 4.** Singleplex and multiplex STR amplification performed on the PCR-CE microsystem. (A) Amplification of the amelogenin marker from male standard genomic DNA. A 106-bp X-chromosome and a 112-bp Y-chromosome amplicon labeled with FAM-FAM were amplified from 20 copies of the template with 32 PCR cycles. (B) DYS390 Y-chromosome amplicon (171 bp) labeled with FAM-R6G from standard male genomic DNA. (C) A 123-bp DYS393 amplicon from male standard genomic DNA labeled with FAM-TMR. (D) A 191-bp DYS439 amplicon labeled with FAM-ROX. (E) Multiplex PCR of all four loci from 50 template copies with 35 PCR cycles.

of this marker produces a 106-bp and a 112-bp amplicon from the X and Y chromosomes, respectively. Amelogenin is widely used for sex-typing and sample quality evaluation in the forensic community.<sup>35</sup> In our system, amelogenin serves as a positive control, providing important information about sample quality and amplification performance.

**Singleplex and Multiplex STR Amplification.** Singleplex amplifications on each locus were performed first to examine the functionality of the PCR-CE microsystem as well as the amplification performance of these DNA markers. In these PCR experiments, each DNA marker was amplified from 20 copies of 9948 male standard genomic DNA templates in the 160-nL PCR chamber with 32 PCR cycles. After thermal cycling, the PCR product was immediately injected and separated on the electrophoresis channel. An entire analysis was completed in 1.5 h. Panel A in Figure 4 presents an amplification of the amelogenin marker. A 106-bp X-chromosome and a 112-bp Y-chromosome amplicon labeled with FAM-FAM were observed, indicating that the template is male DNA as expected. Panel B presents an amplification and detection of the DYS390 locus, revealing a 171-bp

(33) Medintz, I. L.; Berti, L.; Emrich, C. A.; Tom, J.; Scherer, J. R.; Mathies, R. A. *Clin. Chem.* **2001**, *47*, 1614-1621.

(34) Kayser, M.; Kittler, R.; Erler, A.; Hedman, M.; Lee, A. C.; Mohyuddin, A.; Mehdi, S. Q.; Rosser, Z.; Stoneking, M.; Jobling, M. A.; Sajantila, A.; Tyler-Smith, C. *Am. J. Hum. Genet.* **2004**, *74*, 1183-1197.

(35) Sullivan, K. M.; Mannucci, A.; Kimpton, C. P.; Gill, P. *Biotechniques* **1993**, *15*, 637-641.



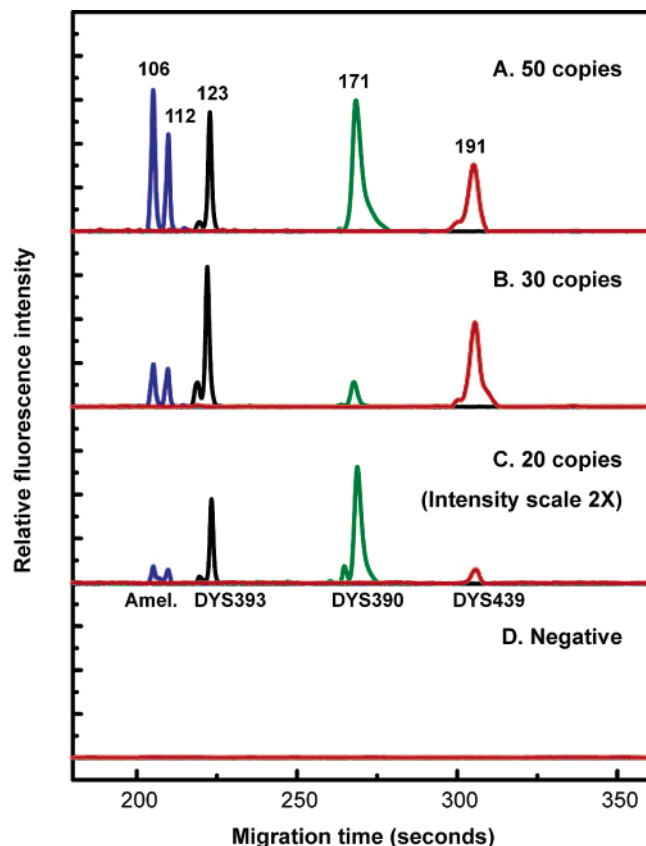


**Figure 5.** Limit of detection for multiplex analyses of 9948 male standard genomic DNA using the PCR–CE microdevice. PCR cycles were 35 in each case. The trace obtained from 20 template copies was enlarged twice for display. A negative control experiment was performed to confirm the absence of carryover.

amplicon labeled with FAM-R6G. Similarly, a 123-bp DYS393 amplicon labeled with FAM-TMR and a 191-bp DYS439 amplicon labeled with FAM-ROX were obtained, respectively, in panels C and D. With optimized primer concentrations (150 nM amelogenin, 80 nM DYS390, 120 nM DYS393, and 180 nM DYS439), each DNA marker demonstrated a similar amplification efficiency and good sensitivity.

Following successful amplifications on each locus individually, a multiplex PCR–CE experiment was carried out on this four-locus multiplex system. Starting template (50 copies of 9948 male standard genomic DNA) was loaded in the PCR chamber, and 35 PCR cycles were performed. Primer concentrations used in the multiplex system were adjusted slightly to maintain balanced peak intensities for each locus (150 nM for amelogenin, 150 nM for DYS390, 120 nM for DYS393, and 180 nM for DYS439). As shown in Figure 4 (panel E), all the peaks (106, 112, 123, 171, and 191 bp) were fully resolved and balanced. Compared with singleplex amplifications, multiplex STR amplifications exhibit lower amplicon yields due to competition between each locus. Therefore, both the initial template copy number (50 copies) and the PCR cycle number (35 cycles) were increased to compensate for this effect.

A limit-of-detection analysis for multiplex amplification of 9948 male standard genomic DNA was performed. Figure 5 presents results from a series of amplifications conducted from 0, 20, 30, and 50 copies of template in the PCR chamber with 35 PCR cycles.

Even with only 20 copies of DNA template, the multiplex amplification still shows all the expected peaks in the electropherogram. An amplification from 10 copies was also performed; however, a complete profile was not obtained. The amplicon peak intensities are reduced and show more variability as the initial templates decrease from 50 to 20 copies. When the template copy numbers fall into the low copy number amplification range (<100 pg or <33 copies),<sup>2</sup> stochastic effects occur, and repeated amplifications of identical solutions exhibit fluctuations in peak intensity. Finally, it should be noted that the absence of any amplicons in the negative control (0 initial copies) demonstrates the effectiveness of the piranha cleaning conducted after each run.

**Analysis of Forensic Casework.** Samples obtained from forensic casework usually have lower amplification efficiency, due to PCR inhibitors, which remain with the DNA throughout the sample preparation process,<sup>36,37</sup> or due to DNA degradation by exposure to environmental elements or natural contaminants.<sup>38</sup> Here we selected two typical samples, one from an oral swab and the other from human bone, which were previously processed and analyzed by the Palm Beach County Sheriff's Office. Buccal cell collection with a cotton oral swab is often used in cases where reference samples from suspects or family members are needed to perform comparative DNA testing.<sup>39</sup> Human bone remains in forensic casework represent one of the most degraded biological materials for PCR-based DNA typing, since they are usually collected after a long period of exposure in a harsh environment, such as burial in soil.<sup>40</sup> Therefore, these two typical samples were chosen to test our integrated PCR–CE forensic system.

Four separate amplifications, including 9948 male and 9947A female standard genomic DNA, which serve as controls, and two casework samples from an oral swab and human bone, were conducted from 50 template copies with 35 PCR cycles. Panels A and B in Figure 6 present the PCR analyses conducted from male and female standard DNA, showing all the expected peaks with correct gender discrimination. Figure 6C presents an amplification and analysis of the DNA sample extracted from an oral swab. All the amplicons in four loci were successfully obtained, indicating the sample is male DNA. Figure 6D shows only one peak at 106 bp, corresponding to the successful amplification of female human bone DNA. Off-chip results using an ABI Prism 3100 confirmed the genders of these two samples and indicated that the amplicon lengths of the oral swab sample in DYS390 and DYS439 are 167 and 187 bp, one repeat less than those corresponding amplicons from 9948 standard DNA. These differences were also observed in the on-chip results, by aligning the profiles of the male standard DNA and the oral swab sample.

**Mixture Analysis.** The ability of our system to provide interpretable DNA amplification profiles, when a minute amount of male DNA is present in a high background of female DNA, is very critical, as this situation is often encountered in Y-STR forensic analysis.<sup>6</sup> Quadruplex amplification and detection was

(36) Wilson, I. G. *Appl. Environ. Microbiol.* **1997**, *63*, 3741–3751.

(37) Radstrom, P.; Knutsson, R.; Wolffs, P.; Lovenklev, M.; Lofstrom, C. *Mol. Biotechnol.* **2004**, *26*, 133–146.

(38) Bar, W.; Kratzer, A.; Machler, M.; Schmid, W. *Forensic Sci. Int.* **1988**, *39*, 59–70.

(39) Burger, M. F.; Song, E. Y.; Schumm, J. W. *Biotechniques* **2005**, *39*, 257–261.

(40) Opel, K. L.; Chung, D. T.; Drabek, J.; Tatarek, N. E.; Jantz, L. M.; McCord, B. R. *J. Forensic Sci.* **2006**, *51*, 351–356.



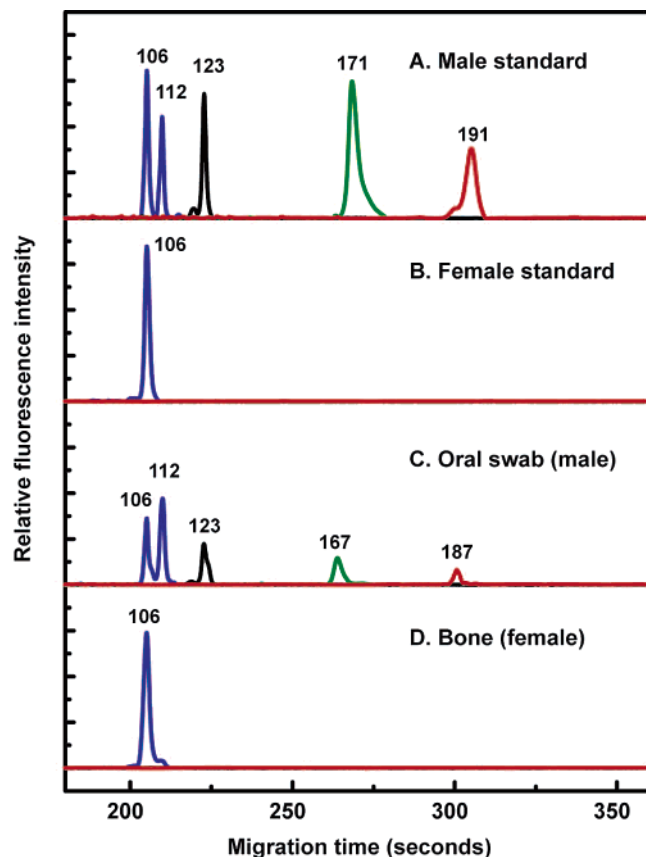


**Figure 6.** Multiplex STR forensic analysis using the PCR–CE microdevice conducted from standard genomic DNA and from samples extracted from an oral swab and human bone, respectively. In each case, 50 starting template copies and 35 PCR cycles were employed. (A) Analysis conducted from 9948 male standard DNA, showing the presence of all the amplicons on these four loci. (B) Analysis of 9947A female standard DNA, showing only the expected presence of the 106-bp X-chromosome peak. (C) Analysis conducted on genomic DNA extracted from an oral swab. All the expected peaks were observed, showing the source is male. (D) Analysis of a human bone sample. Only one 106-bp amplicon was detected, showing the source is female.

carried out by mixing male and female standard genomic DNA together during the sample preparation. The male DNA in each run was maintained at 50 copies, while the female DNA was increased to achieve ratios of male-to-female genomic DNA of 1:1, 1:5, and 1:10, respectively, resulting in ratios of Y-to-X chromosomes of 1:3, 1:11, and 1:21. Since a high yield of the 106-bp X-chromosome product is expected to overwhelm the other Y-chromosome amplicons, the DNA polymerase concentration was increased from 0.2 to 0.4 unit/ $\mu$ L to ensure full amplification and to produce balanced profiles. The results of this experiment in Figure 7 show that, as the ratio increased, the 106-bp amplicon from X chromosome became more and more dominant over the 112-bp Y-chromosome product. The peak area ratios are roughly equal to the initial template ratios of Y-to-X chromosomes (1:3, 1:11, and 1:21). The other three Y-chromosome loci (DYS390, DYS393, and DYS439) were still fully amplified and balanced in each case. However, slight signal reductions were observed, due largely to the increase of the 106-bp X-chromosome amplicon, which used up most of the PCR resources. These data indicate that the system is capable of analyzing male DNA in the presence

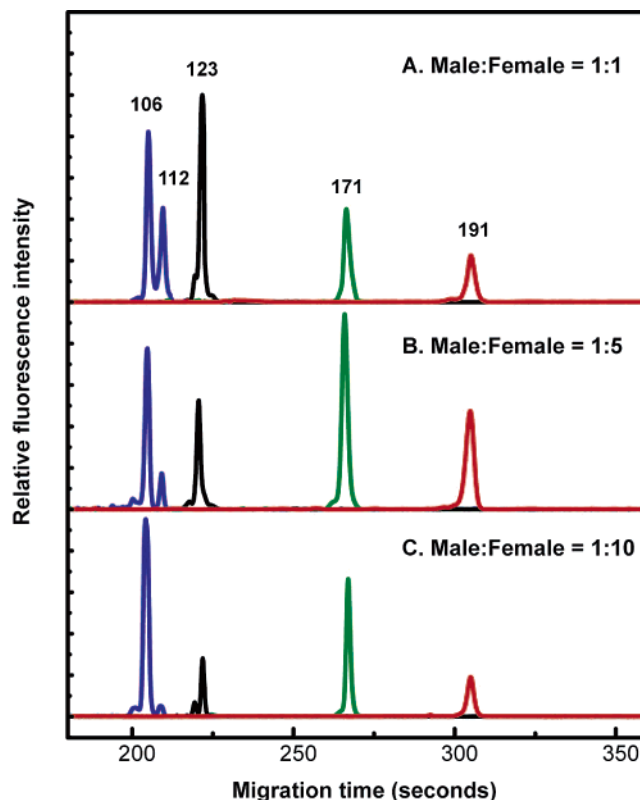


**Figure 7.** Multiplex STR analysis of male genomic DNA (50 copies) in the presence of a female genomic DNA background using the PCR–CE microsystem (35 PCR cycles). The template ratios of male-to-female range from 1:1 to 1:10. As the ratio increased, the 106-bp amelogenin amplicon from the X-chromosome became more and more dominant over the 112-bp Y-chromosome product.

of a high female DNA background. Although the ratio could be lowered further in amplifications without the amelogenin marker, additional valuable information, such as the male-to-female DNA ratio, is obtained with this quadruplex system from the peak area ratio of the two peaks in amelogenin.

## CONCLUSIONS

A fully integrated PCR–CE microdevice has been optimized for forensic analysis and combined with a new portable instrument including controls for chip operation and four-color fluorescence detection. This system was used to perform a quadruplex STR forensic analysis; the entire assay was finished in 1.5 h due to the rapid low-volume (160 nL) thermal cycling and integrated high-speed electrophoretic separation. The detection limit of this system for multiplex amplification of genomic DNA is as low as 20 copies in the PCR chamber. Two real-world forensic casework samples extracted from an oral swab and human bone were successfully analyzed, showing the practical application of this system. Finally, male genomic DNA was tested in the presence of excess female genomic DNA background. Intense balanced peaks were observed even at the male-to-female DNA ratio of 1:10.

This microdevice presents a first and significant step toward a fully integrated and portable system allowing highly sensitive, rapid STR analyses in a setting outside a forensic laboratory. For practical forensic applications in the future, a co-injection structure can be included in the microdevice to facilitate running sizing and allelic ladders,<sup>26</sup> and more STR loci should be included to improve

the discrimination power. Additionally, autosomal STR typing is under investigation to extend the application range of the portable microsystem. The integrated, high-speed and low-volume STR typing methods developed here will accelerate the forensic identification process and lower the assay cost, thereby reducing backlogs and advancing forensic DNA applications. Furthermore, our demonstration of successful STR analyses on a portable PCR–CE system validates the concept of point-of-analysis DNA typing in crime scene, mass disaster, or security checkpoint applications, where rapid on-site human identification is demanded.<sup>5,41,42</sup>

#### ACKNOWLEDGMENT

We thank the UC Berkeley Chemistry Machine Shop for construction of the portable analysis instrument, and Henry Chan of the UC Berkeley Chemistry Electronic Shop for design and fabrication of the electronics. PCR–CE chip microfabrication was

conducted at the University of California, Berkeley Microfabrication Laboratory. We thank Amy McGuckian and Cecelia Crouse at the Palm Beach County Sheriff's Office for providing the forensic casework samples and Stephanie Yeung and Susan Greenspoon for valuable discussions. We also thank John M. Butler at the National Institute of Standards and Technology for providing the U.S. population data on the three Y-STR loci. This project was supported by Grant 2004-DN-BX-K216 awarded by the National Institute of Justice, Office of Justice Programs, U.S. Department of Justice. Points of view in this document are those of the authors and do not necessarily represent the official position or policies of the U.S. Department of Justice. R.A.M. has a financial interest in Microchip Biotechnologies, Inc. that is commercially developing aspects of the technologies presented here.

(41) Primorac, D.; Schanfield, M. S.; Primorac, D. *Croat. Med. J.* **2000**, *41*, 32–46.

(42) Belgrader, P.; Smith, J. K.; Weedn, V. W.; Northrup, M. A. *J. Forensic Sci.* **1998**, *43*, 315–319.

Received for review October 18, 2006. Accepted November 30, 2006.

AC061961K